TÜBİTAK

Research Article

Turk. J. Vet. Anim. Sci.
2009; 33(2): 105-111
© TÜBİTAK
doi:10.3906/vet-0705-22

Magnetic Resonance Imaging Findings of Intracranial Tumors in Dogs: A Review of 26 Cases

Ömer BEŞALTI[1], Y. Sinan ŞİRİN[2], Zeynep PEKCAN[3], Gonca ERBAŞ[4]

[1]Department of Surgery, Faculty of Veterinary Medicine, Ankara University, Ankara - TURKEY

[2]Department of Surgery, Faculty of Veterinary Medicine, Ondokuz Mayıs University, Samsun - TURKEY

[3]Department of Surgery, Faculty of Veterinary Medicine, Kırıkkale University, Kırıkkale - TURKEY

[4]Department of Radiology, Faculty of Medicine, Gazi University, Beşevler, Ankara - TURKEY

Received: 29.05.2007

Abstract: The aim of this study was to report the magnetic resonance imaging (MRI) findings of intracranial tumors in 26 dogs. The medical records of dogs admitted to the Department of Surgery, Faculty of Veterinary Medicine, Ankara University for central nervous system disorders were reviewed, and dogs with intracranial tumors that were diagnosed with MRI between November 1997 and June 2006 were included in the study.

MR images were obtained as T1 weighted (T1W), T2 weighted (T2W), and contrast enhanced T1 weighted (following Gd-DTPA administration) in the transverse, coronal (dorsal), and sagittal planes. The following features were evaluated in order to characterize the lesions and to establish diagnoses based on radiological findings: site of origin, anatomic location, signal characteristics on T1W and T2W images, contrast enhancement, shape and size, number (multiple or single), and presence of edema and midline shift.

The radiological diagnoses were as follows: intracranially invading sinus tumor (n = 3), meningioma (n = 7), choroid plexus tumor or ependymoma (n = 3), ependymoma (n = 1), glioma (n = 5), metastatic tumor (n = 3), astrocytoma (n = 1), astrocytoma or metastasis (n = 1), cavernoma (n = 1), and hypophyseal adenoma (n = 1). In conclusion, lesions occupying the intracranial space can be accurately diagnosed and tumor type can be predicted with MRI.

Key Words: Brain tumor, dog, magnetic resonance imaging

Köpeklerde İntrakranial Tümörlerin Manyetik Rezonans Görüntüleme Bulguları: 26 Olgu

Özet: Bu çalışmanın amacı 26 köpekte rastlanan intrakranial tümörün manyetik rezonans görüntüleme (MRG) bulgularını sunmaktır. Kasım 1997- Haziran 2006 tarihleri arasında Ankara Üniversitesi Veteriner Fakültesi Cerrahi Anabilim Dalına merkezi sinir sistemi hastalığı nedeniyle getirilen ve MRG ile intrakranial tümör tanısı konulan köpekler çalışma kapsamına alındı.

Manyetik rezonans görüntüleri, T1 ağırlıklı (T1W), T2 ağırlıklı (T2W) ve kontrastlı T1 ağırlıklı (GD-DTPA uygulaması sonrasında) transversal, koronal ve sagittal kesitler şeklinde alındı. Köken aldığı bölge, anatomik lokalizasyon, T1W ve T2W görüntülerdeki sinyal karakteristiği, kontrast artışı, şekli ve boyutları, sayısı (tek veya çok), ödemin varlığı ve yer değiştirme gibi özellikler, lezyonun karakterini belirlemek ve radyolojik bulgulara göre tanı koyabilmek için incelendi.

Radyolojik tanıya göre intrakraniale invaze sinus tümörü (n = 3), meningioma (n = 7), kroid pleksus tümörü veya ependimoma (n = 3), ependimoma (n = 1), glioma (n = 5), metastatik tümör (n = 3), astrostoma (n = 1), astrostoma veya metastaz (n = 1), kavernoma (n = 1) ve hipofiz adenoma (n = 1) belirlendi. Sonuç olarak, MRG ile intrakranial kitlelerin tam olarak tespit edilebileceği ve tümör tipinin tahmin edilebileceği belirlendi.

Anahtar Sözcükler: Beyin tümörü, köpek, manyetik rezonans görüntüleme

* E-mail: besalti@hotmail.com

Introduction

Intracranial tumors occur frequently in dogs, with a reported incidence rate of approximately 3.0%, although the actual incidence is unknown (1,2). Many types of brain tumors have been reported in dogs, and meningiomas and gliomas are the 2 most common. Most canine brain tumors are primary, whereas secondary or metastatic tumors are reported less frequently (2,3).

The availability of advanced imaging techniques enhances our understanding and knowledge about the incidence of brain tumor types (4-7). Magnetic resonance imaging (MRI) is the only diagnostic tool available for the ante-mortem prediction of the various histological types of brain neoplasms (8,9). Characteristic MRI findings of some tumors serve as valuable clues for reaching a tentative diagnosis (10). This imaging modality is instrumental in choosing appropriate treatment and patient management protocols (5,11).

This retrospective study was designed to determine the frequency of canine brain tumors and to report the related MRI findings in our patient group.

Materials and Methods

Medical records of dogs seen in our Department between November 1997 and June 2006 were reviewed retrospectively to identify those that underwent MRI examination for a probable intracranial mass. Cases with intracranial tumors were included in this study. Demographic information, including age, breed, and sex were obtained from the medical records.

All the MR images were acquired with the same 1.5 Tesla MRI unit using a head coil 30 cm in diameter†. T1 (TR: 400-600 ms, TE: 15-20 ms) and T2 (TR: 3500-4500 ms, TE: 90-110 ms) weighted images were obtained. Slice thickness was 3-4 mm and the interslice gap was 0.1 mm.

Contrast enhanced T1W images were obtained after intravenous administration of 0.1 mmol/kg of Gd-DTPA‡. Transverse, coronal (dorsal), and sagittal sections were interpreted to evaluate the tumors under the supervision of a specialist certified in human imaging (GE). Contrast enhancement of the tumors was qualitatively classified into 4 categories: none, mild, moderate, and intense. The following features were recorded: site of origin (extra-axial or intra-axial), anatomic location, T1W and T2W features (iso-, hypo-, or hyperintense relative to brain parenchyma), edema (high signal intensity surrounding the lesion on T2W images, were noted as: none, mild, moderate, and extensive), contour characteristics (regular or irregular), number of lesions (multiple or solitary), and midline shift. If a lesion was elliptical, after measurement of the maximum dimensions in 3 orthogonal planes, the following equation was used to calculate its volume (12):

$$\text{Volume} = \frac{4\,\Pi\,(\text{RC}/2 * \text{ML}/2 * \text{DV}/2}{3}$$

The volumes of spherical masses were calculated with the following equation: $4/3\prod r^3$ (key: RC = rostrocaudal, ML = mediolateral, DV = dorsoventral, and r = radius).

Results

In all, 26 dogs met the selection criteria. There were 12 female and 14 male patients aged between 2.5 and 15 years (mean: 8.1 years). Breed distribution was as follows: 6 Boxers, 7 Poodles, 4 cross breeds, 2 German Shepherds, 2 Collies, 1 Great Dane, 1 Labrador Retriever, 1 Doberman Pincher, 1 Rottweiler, and 1 Golden Retriever.

Details of the MRI findings are shown in the Table. There were 13 dogs with extra-axial tumors and 13 dogs with intra-axial tumors. In 9 cases there was displacement of the brain structures, or midline shift secondary to peritumoral edema or mass effect; however, midline shift was not accompanied by edema in 2 of the cases. Mild or moderate edema was also seen, without shift, in 7 cases. Solitary brain tumors were seen in 10 cases and 3 dogs had multiple tumors.

Primary brain tumors were diagnosed using MRI in 17 dogs. The radiological diagnoses included meningioma (n = 7), choroid plexus tumor or ependymoma (n = 3), ependymoma (n = 1), glioma (n = 5), and astrocytoma (n = 1). Secondary brain tumors were diagnosed in 8 cases, including intracranially invading sinus tumors (n = 3), a hypophyseal adenoma (n = 1), and a cavernoma (n = 1). There were 3 metastatic tumors. In 1 case MRI findings were not specific enough to differentiate an astrocytoma

† Siemens Superconducting Magnet, field strength of 1.5 tesla Siemens AG Munich, Germany
‡ Magnevist, Schering

Table. MRI findings in 26 dogs with intracranial tumors.

Case no.	Tumor type	Anatomic site	Origin	Shape, volume (mm^3)	Midline shift	Edema	Signal intensity	Other features	Contrast enhancement	M/S	Margins
1	Ependymoma	Foramen of Monro	Extra-axial	Spheroidal 546.75	10 mm	None	T1-iso T2-hyper	Dilated R. lateral vent.	Intense	S	lobulated Regular
2	Metastasis	L. parietal cortex, brain stem, 4th vent.	Intra-axial	Spheroidal 1436.027	-	moderate	T1-hypo T2-hyper	-	Moderate	S	Regular
3	Oligodendroglioma or Metastasis	R. frontal	Intra-axial	Elliptical 3868.48	4 mm	Extensive	T1-hypo T2-hyper	Cyst	Not administered	S	Irregular
4	Choroid plexus tumor	3rd vent.	Intra-axial	Elliptical 6280	-	Moderate	T1-iso T2-hyper	Calcification	Moderate	S	Irregular
5	Meningioma	L. frontal-basal	Extra-axial	Elliptical 6556.32	5 mm	None	T1-iso T2-iso	-	Intense	S	Regular
6	Glioma	R. lentiform nucleus	Intra-axial	Spheroid 904.32	-	Mild	T1-hypo T2-hyper	-	Moderate	S	Regular
7	Glioma	R. frontotemporal	Intra-axial	Spheroid 3589.543	-	Moderate	T1-hypo T2-hyper	-	None	S	Irregular
8	Meningioma	Median sphenoid	Extra-axial	Elliptical 4850.777	-	None	T1-hypo T2-hyper	Dilated third vent.	Intense	S	Regular lobulated
9	Choroid Plexus tumor	3rd vent.	Intra-axial	Elliptical 549.5	-	None	T1-hypo T2- hyper	Dilatation of lateral vent.	Intense	S	Regular lobulated
10	Glioma	L. frontotemporal	Intra-axial	Elliptical 15.7	4 mm	Extensive	T1-hypo T2-hyper	-	None	S	Irregular
11	Sinus tumor	Frontal sinus ethmoid cells, L. frontal lobe	Extra-axial	Elliptical 33,409.60	-	Mild	T1-iso T2-iso	Cystic components	Intense	S	Lobulated
12	Cavernoma	R. frontal	Extra-axial	Spheroid 267.947	-	None	T1-hypo T2-hypo	Chronic hemorrhage	None	-	Lobulated
13	Meningioma	L. temporal	Extra-axial	Spheroid 1766.25	8 mm	Extensive	T1-hypo T2-iso	Calcification	Intense	S	Regular
14	Metastasis	Largest R. occipital, parietal	Intra-axial	Spheroid	5 mm	Extensive	T1 hypo T2-iso	Necrosis	Moderate	M n = 8	Regular
15	Meningioma	R. frontal	Extra-axial	Elliptical 4082	5 mm	Extensive	T1-iso T2-iso	-	Moderate	S	Regular
16	Meningioma	R. pontocerebellar angle	Extra-axial	Elliptical 736.85	-	Mild	T1-hypo T2-hyper		Moderate	S	Regular
17	Sinus tumor	L. frontal sinus	Extra-axial	Elliptical 19,258.67	-	Moderate	T1-hypo T2-hyper	-	Mild	S	Regular
18	Astrocytoma	R. frontotemporal	Intra-axial	Spheroid 1766.25	-	None	T1-hypo T2- hyper	Predominantly cystic	Mild	S	Regular
19	Glioma	L. frontal	Intra-axial	Elliptical 489.84	-	Moderate	T1-iso T2-hyper	-	None	S	Irregular
20	Meningioma	Sphenoid basis	Extra-axial	Elliptical 5324.917	-	Moderate	T1-iso T2- hyper	Cysts, necrosis	Intense	S	Lobulated Regular
21	Metastasis	R., L parietal	Intra-axial	Elliptical	4 mm	Moderate	T1-hypo T2- iso	Necrosis Lung mass	Intense	M n = 2	Regular
22	Glioma	R. frontal	Intra-axial	Elliptical 5861.333	3 mm	Mild	T1-hypo T2-hyper	Necrosis	Moderate	S	Irregular
23	Choroid plexus tumor	R. lateral vent.	Intra-axial	Elliptical 3868.48	9 mm	Extensive	T1-iso T2-iso	-	Intense	S	Lobulated Regular
24	Meningioma	L. frontal	Extra-axial	Elliptical 7785.63	4 mm	Mild	T1-iso T2-iso	-	Intense	S	Regular
25	Sinus tumor	Bilateral frontal sinus	Extra-axial	Elliptical 73,790	-	None	T1-iso T2-iso	Necrosis	Intense	S	Lobulated Regular
26	Hypophyseal Adenoma	Suprasellar	Extra-axial	Spheroid 6367.397	-	Mild	T1-hypo T2 hyper	-	Ring enhancement	S	Regular

L: Left; R: right; vent: ventricle; M: multiple; S: solitary.

from a metastatic tumor. In all, 17 tumors were elliptical and 9 were spherical.

Radiologically, all meningiomas had dural contact and showed the dural tail sign. These tumors showed extensive contrast enhancement. They were elliptical in axial MR images, except in 1 case (Figure 1). In the case of a meningioma located near the medial sphenoid bone, a third ventricular dilatation was noted. One meningioma contained cystic and necrotic areas, while another was calcified. Meningioma volumes are shown in the Table.

Gliomas were hypointense on T1W images and hyperintense on T2W images. They were spherical in 2 cases and elliptical with irregular margins in 3. Gliomas were associated with midline shift in 2 cases. Mild to extensive edema was depicted in all glioma cases. In 1 case a choroid plexus tumor was located in the lateral ventricle, associated with midline shift and extensive edema. The remaining 2 cases had tumors located in the third ventricle, which were associated with ventricular dilatation and calcification (Figure 2). An ependymoma (n = 1) was located at the foramen of Monro, which was associated with right lateral ventricular dilatation and shift. The margins of the tumor were lobulated and irregular. The tumor was hyperintense on T2W images and intensely enhanced after contrast administration. Intracranially invading sinus tumors were isointense relative to brain parenchyma on both T1W and T2W images. In 2 cases the margins were lobulated, and were associated with necrosis and cysts; however, in 1 case the tumor was hypointense on T1W and hyperintense on T2W images, with well-delineated margins (Figure 3). A cavernoma was seen in 1 case as a lobulated mass with an associated hemorrhage.

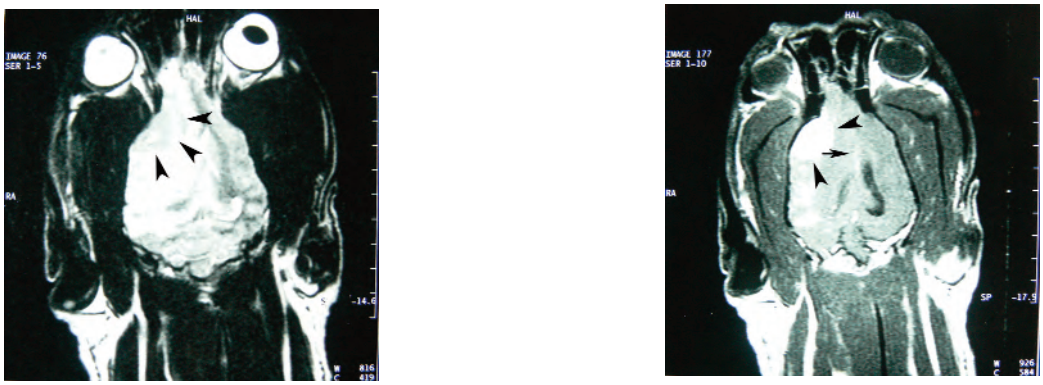

Figure 1. Right frontal meningioma with regular margins and ellipsoid shape (case 15 in the Table). Isointense mass (black arrowheads) and associated hyperintense edema in coronal T2W image (a). Tumor shows moderate contrast enhancement in coronal T1W image (b). Note the midline shift (black arrow).

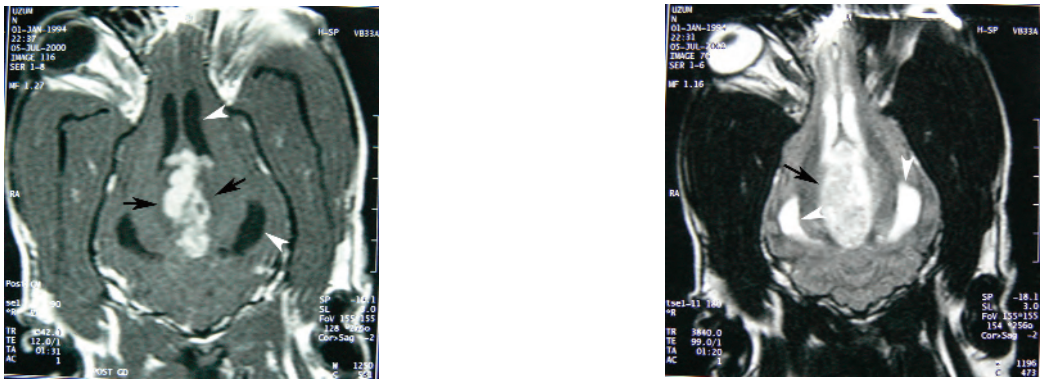

Figure 2. Choroid plexus tumor in the third ventricle with lobulated margins (black arrows) (case 9 in the Table). Intense contrast enhancement in coronal T1W image (a) and hyperintense appearance in coronal T2W image (b). Note the dilatation in both lateral ventricles (white arrowheads).

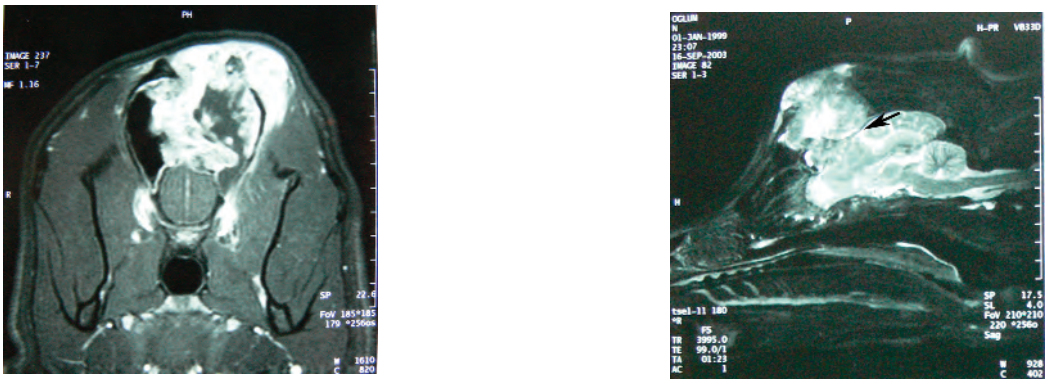

Figure 3. Sinus tumor invading the intracranial space, with lobulated margins and associated necrosis (case 25 in the Table). Intense contrast enhancement in transverse T1W image (a), and intracranial extension and invasion of brain parenchyma in sagittal T2W image (b).

A hypophyseal adenoma was depicted in 1 case as an ovoid mass at the sella, and extended into the parasellar regions. The mass had a heterogeneous signal on T1W images and was hyperintense on T2W images. The mass was intensely enhanced after contrast administration (Figure 4). Macroscopically, the mass was 1 × 1.8 × 1.5 cm in diameter, spherical, firm, and dark brown.

Metastatic tumors were observed in 3 cases, and were associated with edema; in 2 cases there were midline shift and central necrosis. The margins of these tumors were well delineated. In 1 case of a solitary tumor located in the right frontal cortex there were associated edema and shift. This case had a cystic mass and was interpreted as an astrocytoma or metastasis. Another dog had a pulmonary carcinoma metastasis to the brain (Figure 5). In the 2 cases with metastasis there were multiple masses, while the remaining tumors were solitary.

Discussion

Human intracranial tumors can be diagnosed using MRI and CT with an accuracy of up to 85%-90% (7,10). The number of reports describing the MRI findings of intracranial tumors in dogs has increased in recent years, providing more knowledge and widespread familiarity, resulting in the ability to diagnose with similar accuracy as in humans (4-7). Accurate diagnosis of a primary brain tumor using MRI was reported to be 100%, and correct prediction of histological type was reported as 71% (2). Intracranial tumors can be studied in greater detail for specific types of tumors using different MRI techniques, such as magnetic resonance proton spectroscopy (10,13). In the present study conventional MRI techniques (T1W, T2W, and contrast enhanced T1W sequences) were used to evaluate mass lesions. MR signal characteristics, contrast enhancement patterns, anatomic location, and

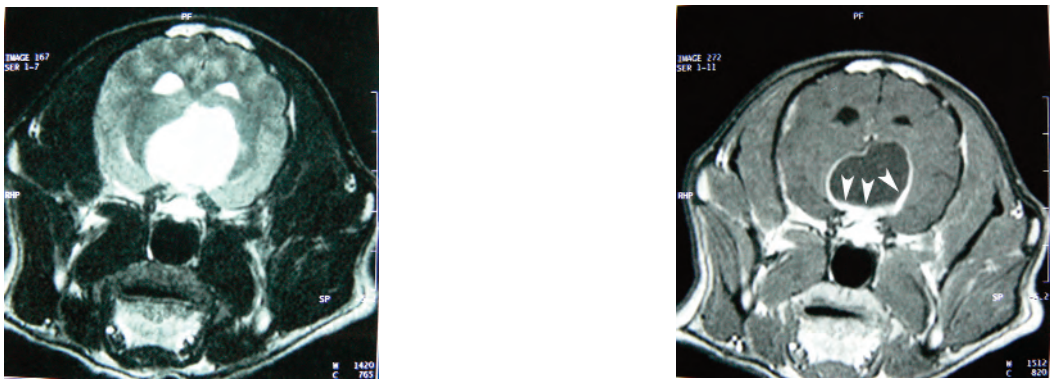

Figure 4. Suprasellar mass in transverse sections; pituitary adenoma (case 16 in the Table). The mass is hyperintense in T2W image (a). Note the ring-like enhancement pattern in the post-contrast T1W image (white arrowheads) (b).

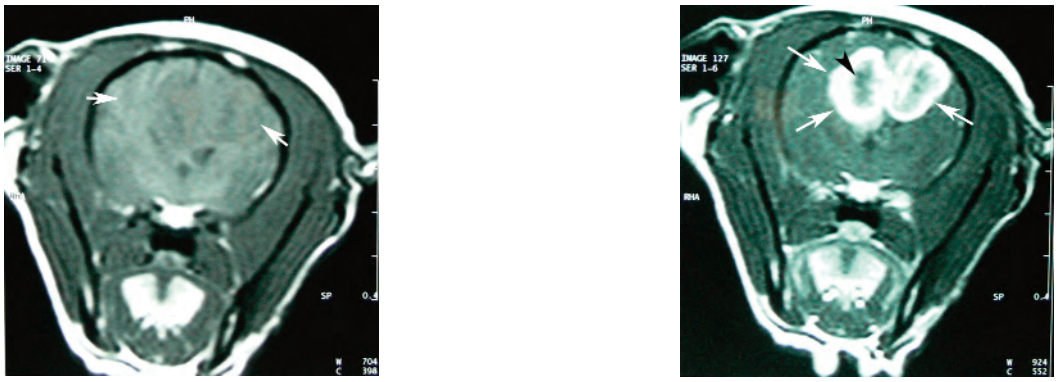

Figure 5. Metastatic tumor with 4-mm midline shift in transverse MR images (case 21 in the Table). Hypointense mass in T1W image (white arrows) (a) and post-contrast T1W image (b). Note the intense contrast enhancement and central necrosis (black arrowhead).

shape of tumors are very important factors in the prediction of tumor types (2,7); however, histopathological examination is essential for making a definitive diagnoses of intracranial tumors. Therefore, CT-guided brain biopsy techniques for animals have been improved (14).

The origin of intracranial tumors is important in determining tumor type. Extra-axial tumors arising from tissues outside the neural axis and intra-axial tumors were observed in equal numbers in the present study. This finding differs from the results of a study carried out by Kraft et al. (7) in which the presence of extra-axial tumors was reported in 68% of the cases.

Anatomic location is a distinctive characteristic of some tumors, such as nasal or pituitary tumors, and ependymoma or choroid plexus tumors. Meningiomas are dura-based tumors with dural contacts showing the dural tail sign. The dural tail sign is usually observed with contrast enhanced CT or MRI, and is suggested to be an indicator of dural origin (10). These classical diagnostic features, which are used in human medicine, can also be accurately applied to dogs.

Intracranial tumors may have mass effect relative to their size, and clinical signs of these tumors are related to this event. Edema, hemorrhage, infarction, hydrocephalus, ventricular dilatation, and midline shift can cause mass effect. Recently, the incidence rate of brain herniation associated with rostrotentorial mass lesions in dogs was reported as 35.30% (54/153) (12). In the present study edema was seen in 18 cases (69.23%). There was edema in 5 meningioma cases (71%) and in all glioma and metastatic cases (100%). Midline shift was also associated with edema in 81.81% of the cases. In the light of these findings, edema can be considered a major factor in the displacement of brain structures. Ventricular dilatation was seen in 1 choroid plexus tumor case, 1 ependymoma case, and 1 meningioma case, due to obstruction of the flow of cerebrospinal fluid. Some characteristic imaging findings, such as calcification, can be related to some tumor types. In the present study 2 calcified masses were observed, as well as 1 meningioma and 1 choroid plexus tumor. All of these imaging characteristics can guide clinicians in determining the appropriate management protocol (7,10,13).

Intracranial tumors, especially primary brain tumors in dogs, are solitary, although multiple brain tumors have been reported in a few cases (3,9,12,15). In the present case series only 2 dogs with metastatic tumors had multiple masses in the brain; the remaining cases had solitary masses. This finding is in accordance with the literature.

Even though tumor location is related to clinical signs, tumor volume can also be related to clinical signs. Because of uncontrollable data (differences in breed, head shape, cranial size, etc.) mass volume could not be evaluated relative to brain diameter or total brain volume; however, tumor volumes in the present study represent approximate values because volume was calculated by measuring MR images.

Although brain tumors occur in all breeds and genders, and at any age, their incidence increases over 5

years of age and in certain breeds (12,16,17). Median age (8.1 years) and gender (12 female and 14 male) of the dogs in the present study were similar to those previously reported (12,17,18). Meningiomas have been reported to be the most common brain tumor, followed by gliomas (2,18). Gliomas have a predilection for brachycephalic breeds (16). The results of the present study regarding breed distribution are similar to previous reports (12,17); more Poodles and Boxers had intracranial tumors than the other breeds seen at our clinic between November 1997 and June 2006. Glial cell tumors were seen in 66.66% of the Boxers included in this case series.

In conclusion, lesions occupying the intracranial space can be accurately diagnosed and tumor type can be predicted using MRI. Even in cases lacking histopathological confirmation, MR findings, such as edema, hemorrhage, infarction, calcification, hydrocephalus, ventricular dilatation, and midline shift, could aid accurate radiological diagnosis and help in determining the appropriate management protocol for the patient.

References

1. Moore, M.P., Bagley, R.S., Harrington, M.L., Gavin, P.R.: Intracranial tumours. Vet. Clin. North Am. Small Anim. Pract., 1996; 26: 759-777.
2. Snyder, J.M., Shofer, F.S., Van Winkle, T.J., Massicotte, C.: Canine intracranial primary neoplasia: 173 cases (1986-2003). J. Vet. Intern. Med., 2006; 20: 669-675.
3. Patnaik, A.K., Kay, W.J., Hurvitz, A.I.: Intracranial meningioma: a comparative pathologic study of 28 dogs. Vet. Pathol., 1986; 23: 369-373.
4. Mellema, L.M., Samii, V.F., Vernau, K.M., LeCouteur, R.A.: Meningeal enhancement on magnetic resonance imaging in 15 dogs and 3 cats. Vet. Radiol. Ultrasound, 2002; 43: 10-15.
5. Cherubini, G.B., Mantis, P., Martinez, T.A., Lamb, C.R., Cappello, R.: Utility of magnetic resonance imaging for distinguishing neoplastic from non-neoplastic brain lesions in dogs and cats. Vet. Radiol. Ultrasound, 2005; 46: 384-387.
6. Graham, J.P., Newell, S.M., Voges, A.K., Roberts, G.D., Harrison, J.M.: The dural tail sign in the diagnosis of meningiomas. Vet. Radiol. Ultrasound, 1998; 39: 297-302.
7. Kraft, S.L., Gavin, P.R., DeHaan, C., Moore, M., Wendling, L.R., Leathers, C.W.: Retrospective review of 50 canine intracranial tumors evaluated by magnetic resonance imaging. J. Vet. Intern. Med., 1997; 11: 218-225.
8. Brawner, W.R., Hathcock, J.T.: Neuroradiology. In: Slatter, D. Ed., Textbook of Small Animal Surgery. 3rd edn. Saunders, 2003; 1118-1131.
9. Polizopoulou, Z.S., Koutinas, A.F., Souftas, V.D., Kaldrymidou, E., Kazakos, G., Papadopoulos, G.: Diagnostic correlation of CT-MRI and histopathology in 10 dogs with brain neoplasms. J. Vet. Med. A Physiol. Pathol. Clin. Med., 2004; 51: 226-231.
10. Osborn, A.G., Hedlund, G.L., Illner, A., Salzman, K.L., Blaser, S.I., Jones, B.V.: Part I- Pathology-based Diagnosis-Section 6: Neoplasms and Tumorlike Lesions In: Osborn, A.G., Ed., Diagnostic Imaging: Brain 1st edn., Amirsys Inc. Utah, 2004; 4-144.
11. Shores, A.: Magnetic resonance imaging. Vet. Clin. North Am. Small Anim. Pract., 1993; 23: 437-459.
12. Walmsley, G.L., Herrtage, M.E., Dennis, R., Platt, S.R., Jeffery, N.D.: The relationship between clinical signs and brain herniation associated with rostrotentorial mass lesions in the dog. Vet. J., 2006; 172: 258-264.
13. Benigni, L., Lamb, C.R.: Comparison of fluid-attenuated inversion recovery and T2-weighted magnetic resonance images in dogs and cats with suspected brain disease. Vet. Radiol. Ultrasound, 2005; 64: 287-292.
14. Koblik, P.D., LeCouteur, R.A., Higgins, R.J., Bollen, A.W., Vernau, K.M., Kortz, G.D., Ilkiw, J.E.: CT-guided brain biopsy using a modified Pelorus Mark III stereotactic system: experience with 50 dogs. Vet. Radiol. Ultrasound, 1999; 40: 434-440.
15. Alves, A., Prada, J., Almeida, J.M., Pires, I., Queiroga, F., Platt, S.R., Varejão, A.S.: Primary and secondary tumours occurring simultaneously in the brain of a dog. J. Small Anim. Pract., 2006; 47: 607-610.
16. LeCouteur, R.A.: Current concepts in the diagnosis and treatment of brain tumors in dogs and cats. J. Small Anim. Pract., 1999; 40: 411-416.
17. Bagley, R.S., Gavin, P.R., Moore, M.P., Silver, G.M., Harrington, M.L., Connors, R.L.: Clinical signs associated with brain tumors in dogs: 97 cases (1992-1997). J. Am. Vet. Med. Assoc., 1999; 215: 818-819.
18. Heidner, G.L., Kornegay, J.N., Page, R.L., Dodge, R.K., Thrall, D.E.: Analysis of survival in a retrospective study of 86 dogs with brain tumors. J. Vet. Intern. Med., 1991; 5: 219-226.